European Review for Medical and Pharmacological Sciences 2018; 22: 3976-3987

Isoflurane reduces endotoxin-induced oxidative, inflammatory, and apoptotic responses in H9c2 cardiomyocytes

S. ZHANG, Y. ZHANG

Department of Anesthesiology, Beijing Friendship Hospital, Capital Medical University, Beijing, P.R. China

Abstract. – OBJECTIVE: To investigate the protective effects of ISO on cardiomyocyte injury induced by lipopolysaccharide (LPS) in H9c2 cells.

MATERIALS AND METHODS: Cell viability was determined using the 3-(4,5-dimethylthiazol-2-yl)-2,5-diphenyltetrazolium bromide (MTT) assay. The activities of LDH and CK in the supernatant of H9c2 cells with different treatments were determined using colorimetric assays to assess the conversion of pyruvic acid to lactic acid by LDH and that of triphosphate and creatine to phosphagen by CK.

RESULTS: ISO significantly enhanced cell viability and alleviated the release of lactate dehydrogenase and creatine phosphate kinase in a dose-dependent manner in H9c2 cells treated with LPS. However, the protective effects of higher doses of ISO (1.4% and 2.1%) had no significant difference. Thus, 1.4% ISO was selected for subsequent experiments. ISO inhibited LPS-induced inflammatory responses, as evidenced by reduced expression of tumor necrosis factor-a, interleukin (IL)-1β, and IL-6; it also attenuated the activation of nuclear factor (NF)-kB p65, and the inhibition of NF-kB p65 DNA-binding activity in H9c2 cells. ISO also suppressed oxidative stress and enhanced antioxidant defense in LPS-treated H9c2 cells, as determined by decreased levels of reactive oxygen species and malondialdehyde, increased production of glutathione reductase, and enhanced superoxide dismutase and glutathione peroxidase activities. Moreover, ISO inhibited LPS-induced H9c2 cell apoptosis, as shown by reduced caspase-3 activity; downregulated expression of the pro-apoptotic procaspase-3, cleaved caspase-3, and Bax; and upregulated expression of the anti-apoptotic Bcl-2.

CONCLUSIONS: These findings indicate that ISO reduced LPS-induced H9c2 cell injury via anti-inflammatory, anti-oxidative, and anti-apoptotic activities; hence, ISO may be an alternative therapy for septic heart injury.

Key Words:
Isoflurane, Lipopolysaccharide, Oxidant, Inflammation, Apoptosis.

Introduction

Sepsis is a complex syndrome associated with the progressive endotoxemic development and leads to multiorgan dysfunction as well as significant morbidity and mortality worldwide[1]. Severe heart failure is one of the major causes of death among patients with sepsis[2]. Accumulating evidence suggests that endotoxin-induced inflammation and apoptosis in cardiomyocytes contribute to the progression of heart failure[3]. Thus, attenuation of cardiac dysfunction by inhibiting inflammation and apoptosis during sepsis could significantly increase life expectancy for septic patients.

Previous studies[4,5] demonstrated that systemic inflammatory responses are initiated by bacterial lipopolysaccharide (LPS) or other microbial components. Once LPS enters into the lymphatic and circulatory system, this molecule binds to Toll-like receptor-4 to express tumor necrosis factor (TNF)-α and activate nuclear factor-κB (NF-κB). The latter is an important transcription factor that regulates the release of numerous inflammatory mediators, such as TNF-α, interleukin (IL)-1β, and IL-6[6,7] in cardiomyocytes. Excessive production of pro-inflammatory cytokines, directly and indirectly, promotes cardiac dysfunction[8]. As a high-energy expenditure organ, the heart is particularly sensitive to LPS-induced oxidative damage[9]. Notably, excessive reactive oxygen species (ROS) can provoke NF-κB activation in LPS-stimulated H9c2 cardiomyocytes[10]. Moreover, oxidative stress promotes cardiomyocyte apoptosis[11] and has been implicated in the pathogenesis of various diseases, including heart failure[12,13]. Also, TNF-α-induced apoptotic responses are involved in the pathogenesis of cardiac diseases. These responses are triggered by the binding of TNF-α to its membrane-bound death receptor TNF-α receptor 1 (TNF-R1)[14].

Corresponding Author: Ye Zhang, MD; e-mail: 13911017272@139.com

The anesthetic isoflurane (ISO) confers anti-inflammatory effects by reducing the release of inflammatory mediators of stimulated mononuclear cells *in vitro*[15] and during LPS-induced experimental endotoxemia *in vivo*[16,17]. Hofstetter et al[18] found that even a brief exposure to ISO could considerably reduce the levels of proinflammatory cytokines in the plasma of endotoxemic rats. Specifically, ISO post-treatment alleviates experimental lung injury through inhibition of NF-κB signaling via anti-inflammatory and anti-apoptotic mechanisms[19]. In addition, ISO exerts anti-inflammatory effects on zymosan-challenged murine Kupffer cells by reducing ROS-mediated NF-κB signaling *in vitro* and *in vivo*[20]. However, the protective effects and underlying mechanisms of ISO on LPS-challenged H9c2 cardiomyocytes remain to be investigated.

In this study, we evaluated the cardioprotective effects of ISO on LPS-stimulated H9c2 cardiomyocytes. ISO significantly improved cell viability and inhibited the activities of lactate dehydrogenase (LDH) and creatine kinase (CK) in LPS-exposed H9c2 cardiomyocytes. ISO also reduced LPS-induced mRNA and protein expression of proinflammatory cytokines (TNF-α, IL-1β, and IL-6) and inhibited the activation and DNA-binding activity of NF-κB p65 in H9c2 cardiomyocytes. Moreover, ISO reversed the increase in the levels of ROS and malondialdehyde (MDA) and the decrease in glutathione reductase (GSH) levels as well as the activities of superoxide dismutase (SOD) and glutathione peroxidase (GPx) in LPS-challenged H9c2 cardiomyocytes. Furthermore, ISO impeded LPS-induced myocardial apoptosis by inhibiting caspase-3 activity; downregulating the expression of procaspase-3, cleaved- caspase-3, and Bax; and upregulating the expression of Bcl-2. Therefore, ISO may be an alternative therapy for septic heart injury.

Materials and Methods

Materials

LPS (*Escherichia coli* 055:B5) was purchased from Sigma-Aldrich (St. Louis, MO, USA). ISO was obtained from Baxter (Baxter Healthcare Corporation, Deerfield, IL, USA). The kits for LDH, CK, MDA, GSH, SOD, and GPx were purchased from the Institute of Jiancheng Bioengineering (Nanjing, China). Rabbit anti-rat NF-κB p65, IκB-α, β-actin, and lamin B antibodies were purchased from Abcam (Cambridge, MA, USA). Rabbit anti-rat procaspase-3, cleaved caspase-3, Bax, and Bcl-2 antibodies were purchased from Cell Signaling Technology (Danvers, MA, USA). All reagents used in this work were from Sigma-Aldrich (St. Louis, MO, USA) unless otherwise mentioned.

Cell Culture and Treatment

Rat H9c2 cardiomyoblasts were obtained from the American Type Culture Collection (ATCC, CRL-1446, Rockville, MD, USA). The cells were maintained in Dulbecco's modified Eagle medium (Gibco, Grand Island, NY, USA), supplemented with 100 μg/mL penicillin, 100 μg/mL streptomycin, 2 mM glutamine, 1 mM HEPES buffer, and 10% fetal bovine serum (Gibco) in a humidified incubator with 5% CO_2 at 37°C. H9c2 cells were incubated overnight before the treatment. After stimulation with or without 10 μg/mL LPS for 4 h, the cells were exposed to ISO for 0.5 h at 2 L/min in a metabolic chamber (Columbus Instruments, Columbus, OH, USA) and continuously cultured to the indicated time points. During the exposure, ISO concentration (0.7%, 1.4%, and 2.1%) was verified by sampling exhaust gas with a Datex Capnomac (SOMA Technology Inc., Cheshire, CT, USA). Cells without ISO treatment were used as controls.

Cell Viability Assay

Cell viability was determined using the 3-(4,5-dimethylthiazol-2-yl)-2,5-diphenyltetrazolium bromide (MTT) assay. The cells were seeded at a density of 5×10^3 cells/well in 96-well plates and treated using methods described in the "*Cell Culture and Treatment*" section. 24 h later, the cell culture medium was replaced with 20 μL of 5 mg/mL MTT (Sigma-Aldrich) solution. After incubation of MTT at 37°C for 4 h, the solution was removed, and the produced formazan was solubilized in 150 μL of dimethyl sulfoxide for 30 min at 37°C. The optical density at 570 nm was read on a Microplate Reader (Molecular Devices, Sunnyvale, CA, USA). Cell viability in the control medium without any treatment was represented as 100%, and the cell viability percentage of each well was calculated against the control.

Determination of LDH and CK Activities

The activities of LDH and CK in the supernatant of H9c2 cells with different treatments were determined using colorimetric assays to assess the conversion of pyruvic acid to lactic acid by LDH and that of triphosphate and creatine to phosphagen

by CK, as previously described[21]. Briefly, the cells were cultured in 96-well plates and treated using methods described in the "*Cell Culture and Treatment*" section. Then, the cells were collected and centrifuged at 400 g for 5 min. The supernatants were used for assessing the activities of LDH and CK. Absorbance values after the colorimetric reaction were measured at 490 nm for LDH and 660 nm for CK using a Microplate Reader (Molecular Devices, San Jose, CA, USA).

Quantitative Real-time Polymerase Chain Reaction (qPCR)

The total RNA from the cells with different treatment was extracted using TRIzol reagent (Invitrogen, Carlsbad, CA, USA), in accordance with the protocol of the manufacturers. cDNA was synthesized using a SuperScript First-Strand Synthesis system (Invitrogen). qPCR was performed with Power SYBR Green PCR Master mix (Applied Biosystems, Foster City, CA, USA) and analyzed using an iQ5 Real-time PCR Detection system and analytical software (Bio-Rad, Hercules, CA, USA). The PCR conditions were as follows: initial denaturation at 94°C for 2 min, followed by 25-35 amplification cycles consisting of denaturation at 94°C for 40 s, annealing at 58°C for 45 s and elongation at 72°C for 1 min. The mRNA expression levels were normalized against glyceraldehyde-3-phosphate-dehydrogenase (GAPDH), and the relative mRNA expression levels were calculated using the $2^{-\Delta\Delta Ct}$ method. Primers used for PCR amplification are as follows: for TNF-α, 5′-CATCTTCTCAAAATTCGAGTGACAA-3′ (forward), and 5′-TGGGAGTAGACA AGGTACAACCC-3′ (reverse); for IL-1β, 5′-CAACCAACAAGTGATATTCTCCAT G-3′ (forward), and 5′-GATCCACACTCTCCAGCTGCA-3′ (reverse); for IL-6, 5′-GAGGATACCACTCCCAACAGACC-3′ (forward), and 5′-AAGTGCATCATCGT TGTTCATACA-3′ (reverse); and for GAPDH, 5′-AACGACCCCTTCATTGAC-3′ (forward), and 5′-TCCACGACATACTCAGCAC-3′ (reverse).

Measurement of Cytokine Production

The levels of TNF-α, IL-1β, and IL-6 in the supernatants of the cells with different treatment were measured using commercially available enzyme-linked immunosorbent assay (ELISA) kits (R&D systems, Minneapolis, MN, USA), according to the manufacturer's instructions. Final results were expressed as pg of cytokine/mL media. The results were representative of three independent experiments.

Western Blot Analysis

The cytosolic and nuclear extracts of H9c2 cells with various treatments were prepared using nuclear extraction reagents (Pierce, Rockford, IL, USA). NF-κB p65 levels were quantified in nuclear fractions. Other protein levels were quantified in cytosolic fractions. The two ultimate cell extracts were separated by electrophoresis using a sodium dodecyl sulfate polyacrylamide gel and, then, transferred to nitrocellulose membranes (Millipore, Billerica, MA, USA). Blotting was performed with primary antibodies targeting NF-κB p65, IκB-α, procaspase-3, cleaved caspase-3, Bax, Bcl-2, lamin B, and β-actin, followed by the horseradish-peroxidase-conjugated secondary antibody. Bands were visualized using the enhanced chemiluminescence kit (Santa Cruz Biotechnology, Santa Cruz, CA, USA) and quantified via densitometry using Molecular Analyst software (Bio-Rad Laboratories, Hercules, CA, USA).

NF-kB DNA-binding Activity Assay

The nuclear extracts of the H9c2 cells with various treatments were prepared with a nuclear extraction kit (Pierce). The DNA-binding activity of NF-κB p65 was measured by the NF-κB p65 Transcription Factor Assay Kit (Active Motif, Carlsbad, CA, USA) in accordance with the instructions of the manufacturer.

Detection of Intracellular ROS

The formation of intracellular ROS was evaluated using a fluorescent probe, 2′,7′-dichlorofluorescein diacetate (DCFH-DA), which readily permeates cells and is hydrolyzed to the fluorescent dichlorofluorescein (DCF) upon interaction with ROS. Briefly, H9c2 cells with different treatments were incubated with 10 μM DCF-DA at 37°C for 30 min in the dark. After that, the cells were washed with PBS thrice in order to eliminate the residual DCFH-DA. Cell fluorescence was measured using 485 nm excitation and 535 nm emission with a fluorescence microplate reader (Saire2; Tecan, Switzerland). Images were prepared with Adobe Photoshop (ver. 8.0). Data were collected and analyzed, and the mean fluorescence intensity of five wells per group was used to determine the ROS content ratio.

Measurement of MDA, GSH, SOD, and GPx

The levels of MDA and GSH, as well as the activities of SOD and GPx in supernatants of the H9c2 cells with different treatments, were measured using

commercial kits according to the manufacturer's instructions. In brief, at the indicated time points, the cells were collected and centrifuged at 400 *g* for 5 min. The supernatants were used for measurement of MDA and GSH levels, as well as SOD and GPx activities. Each sample was run in triplicate.

Flow Cytometry Analysis of Cell Apoptosis

To detect H9c2 cell apoptosis, the Annexin V-fluorescein isothiocyanate (FITC) Apoptosis kit (BD Bioscience, San Jose, CA, USA) was used. After the different treatments, H9c2 cells were collected, centrifuged, and resuspended in the binding buffer. Approximately 10 μL of the prepared Annexin V-FITC was added to the mixture, incubated at 37°C for 15 min, and counterstained with 5 μL of propidium iodide (PI) in the dark for 30 min. Following the addition of Annexin V-FITC and PI, the cells were assayed by BD FACSCalibur flow cytometry (BD Bioscience). Results were analyzed by CellQuest software (BD Bioscience, Franklin Lakes, NJ, USA).

Nucleosomal Fragmentation Assay

The apoptosis of H9c2 cells with different treatment was quantified by a nucleosomal fragmentation kit (Cell Death Detection ELISA PLUS; Roche Applied Science, Indianapolis, IN, USA) according to the protocol of the manufacturer. The absorbance values were normalized concerning the control-treated cells to derive a nucleosomal enrichment factor.

Mitochondrial Membrane Potential Analysis

The loss of mitochondrial potential was measured by using the polychromatic 5,5′,6,6′-tetrachloro-1,1′,3,3′-tetraethylbenzimidoazolyl-carbocyanio iodide (JC-1; MitoPT, Immunohistochemistry Technologies, Bloomington, MN, USA). The H9c2 cells were stained with JC-1, which exhibits potential-dependent accumulation in the mitochondria. This aggregation changes the fluorescence properties of JC-1, leading to a shift from green to red fluorescence. At low membrane potentials, JC-1 is present as a monomer and produces green fluorescence (emission at 527 nm). At high membrane potentials or concentrations, JC-1 forms J aggregates (emission at 590 nm) and produces red fluorescence. Fluorescence was measured in a fluorescent plate reader (Bio-Tek, Winooski, VT, USA).

Terminal Deoxynucleotidyl Transferase (TdT)-mediated dUTP Nick-end Labeling Assay

Apoptosis was detected using TdT-mediated dUTP nick-end labeling (TUNEL) method with a commercially available *in situ* apoptosis detection kit (Roche, Basel, Switzerland), according to the manufacturer's instructions. In brief, after the cells were subjected to control or ISO treatment for the indicated time periods, the culture medium was discarded and cells were washed with PBS (pH 7.4). Cells were then fixed with 4% paraformaldehyde for 1 h and incubated with PBS consisting of 0.1% Triton X-100 and 0.1% sodium citrate at 4°C for 5 min. The specimens were then washed with PBS and added to TUNEL detection buffer for incubation at 37°C for 1 h in the dark. TUNEL-positive cells were identified with a fluorescence microscope under an excitation wavelength of 450-500 nm and a detection wavelength of 515-565 nm (green). The percentage of apoptotic cells was calculated by dividing TUNEL-positive cells by the total number of cells visualized in the same field. Experiments were performed in triplicate.

Caspase-3 Activity Assay

The activity of caspase-3 in the cells with different treatment was measured by the Caspase 3 Activity kit (Biovision, Palo Alto, CA, USA). The colorimetric assays were based on the hydrolysis of the amino acid chain acetyl-Asp-Glu-Val-Asp p-nitroanilide (Ac-DEVD-pNA), resulting in the release of the pNA. To detect the activity of caspase-3, the proteolytic reactions were carried out in extraction buffer containing 200 μg of cytosolic protein extract and 40 μM Ac-DEVD-pNA. The reaction mixtures were incubated at 37°C for 2 h and the formation of pNA was measured at 405 nm using a microplate reader (Bio-Tek, Winooski, VT, USA). The results were expressed as the fold-change compared with the control.

Statistical Analysis

The data are expressed as the mean ± standard derivation (SD). One-way ANOVA analysis was used to assess significant differences between the groups, followed by Dunnett's post-hoc test. Statistical calculations were performed using SPSS 16.0 software (SPSS, Inc., Chicago, IL, USA). $p < 0.05$ was considered as statistically significant difference.

Results

ISO Protected H9c2 Cardiomyocytes Against LPS-induced Injury

We investigated the effects of ISO on the viability of LPS-challenged H9c2 cells by using the MTT assay. As shown in Figure 1A, H9c2 cells treated with LPS exhibited significantly reduced cell viability compared with the control. However, cells treated with different ISO concentrations (0.7%, 1.4%, and 2.1%) presented significantly enhanced cell viability compared with LPS-treated cells in a dose-dependent manner. To investigate the protective effects of ISO on LPS-stimulated H9c2 cells, we further assessed the activities of LDH and CK, which are key indicators of cardiomyocyte damage. LDH and CK activities were significantly lower in H9c2 cells treated with ISO (0.7%, 1.4%, and 2.1%) than those in cells stimulated with LPS only (Figures 1B and 1C). LPS-challenged cells treated with 1.4% and 2.1% of ISO showed no significant differences in cell viability and LDH and CK activities (Figure 1A-C). Therefore, 1.4% ISO was selected for subsequent experiments. These results suggested that ISO inhibited LPS-induced damage in H9c2 cardiomyocytes.

ISO Reduced LPS-induced Proinflammatory Cytokine Production in H9c2 Cardiomyocytes

To investigate whether ISO ameliorated inflammatory responses in H9c2 cardiomyocytes

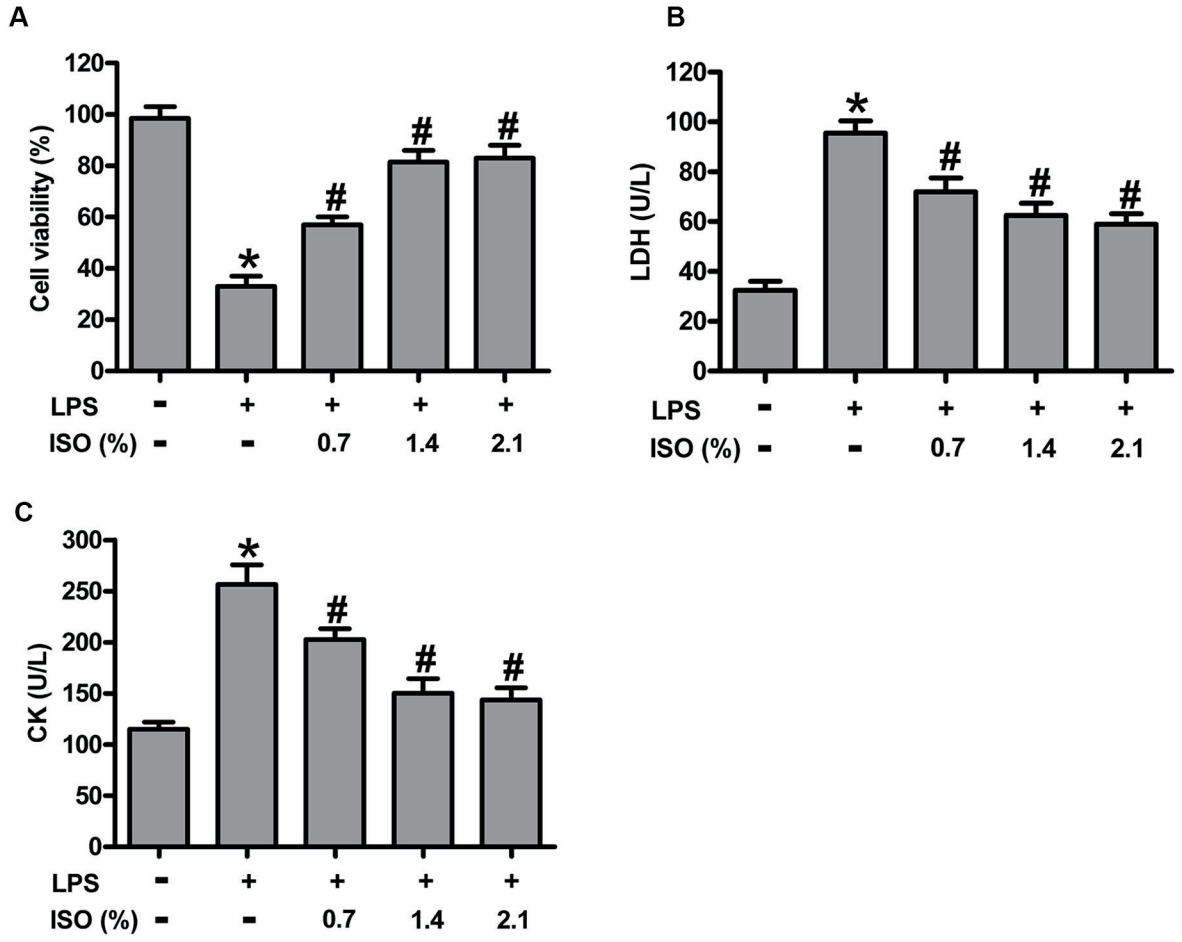

Figure 1. Effects of ISO on cell viability and LDH and CK activities in LPS-challenged H9c2 cardiomyocytes. At 4 h after with or without LPS (10 μg/mL) treatment, the H9c2 cells were exposed to different concentration of ISO (0, 0.7%, 1.4%, and 2.1%) for 0.5 h. At 24 h after with or without LPS treatment, cell viability and the activities of LDH and CK were measured. (A) Cell viability was assessed by MTT assay after treatment with different ISO concentrations. The activities of LDH (B) and CK (C) were determined in the extracellular medium. Data were obtained from three independent experiments and expressed as mean ± SD. *$p < 0.05$ *vs.* − LPS group. $^{\#}p < 0.05$ *vs.* + LPS group.

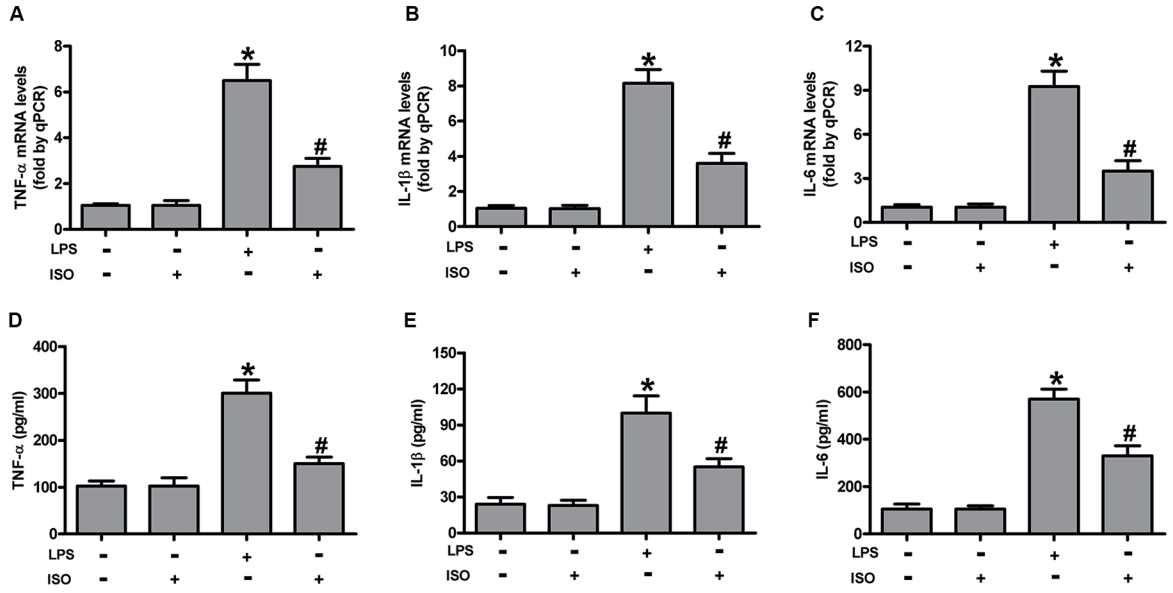

Figure 2. ISO inhibited mRNA and protein expression of proinflammatory cytokines in LPS-stimulated H9c2 cardiomyocytes. At 4 h after with or without LPS (10 μg/mL) treatment, the H9c2 cells were exposed to ISO (0 and 1.4%) for 0.5 h. At 12 h after with or without LPS treatment, the mRNA expression levels of TNF-α (A), IL-1β (B), and IL-6 (C) were assessed by qPCR analysis. At 24 h after with or without LPS treatment, the release of TNF-α (D), IL-1β (E), and IL-6 (F) in the supernatants of the cells with different treatments was evaluated using ELISA. Data were obtained from three independent experiments and expressed as mean ± SD. $^{*}p < 0.05$ *vs.* − LPS group. $^{\#}p < 0.05$ *vs.* + LPS group.

stimulated by LPS, we determined the mRNA and protein expression of TNF-α, IL-1β, and IL-6 through qRT-PCR and ELISA. The mRNA levels of TNF-α (Figure 2A), IL-1β (Fig. 2B), and IL-6 (Figure 2C) in H9c2 cells significantly increased in the presence of LPS. By contrast, the upregulated mRNA expression of TNF-α, IL-1β, and IL-6 was reduced by the ISO treatment (Figure 2A-C). Consistently, the enhanced release of TNF-α (Figure 2D), IL-1β (Figure 2E), and IL-6 (Figure 2F) in the supernatant of LPS-stimulated H9c2 cells was reduced by the ISO treatment. These results indicated that ISO inhibited LPS-induced increase in the mRNA and protein expression of proinflammatory cytokines in H9c2 cells.

ISO Inhibited NF-kB Activation in LPS-stimulated H9c2 Cardiomyocytes

To confirm whether NF-κB is involved in ISO-mediated anti-inflammatory effect in LPS-stimulated H9c2 cells, we conducted Western blot analysis to assess the expression of IκB-α in the cytosol and NF-κB p65 in the nucleus of LPS-treated H9c2 cells in the presence of ISO. IκB-α expression was downregulated in the cytosol (Figure 3A and B), whereas NF-κB p65 expression was considerably upregulated in the nucleus of H9c2 cells in response to LPS exposure (Figure 3C and D); changes in the expression levels of these proteins were reversed by the ISO treatment (Figure 3A-D). Furthermore, the ISO treatment significantly inhibited NF-κB p65 DNA-binding activity in LPS-challenged H9c2 cells, as assessed by the TransAM NF-κB transcription factor assay (Figure 3E). These findings suggested that ISO treatment attenuated LPS-induced NF-κB activation in H9c2 cells.

ISO Ameliorated LPS-induced Oxidative Stress and Enhanced Antioxidant Defense in H9c2 Cardiomyocytes

LPS-induced inflammation can trigger oxidative stress and diminish cellular antioxidant capacity. As shown in Figure 4, the levels of ROS (Figure 4A) and MDA (Figure 4B) increased in H9c2 cells treated with LPS. By contrast, ISO reduced the increase in ROS and MDA production. In addition, reduced production of GSH (Figure 4C) and activities of SOD (Figure 4D) and GPx (Figure 4E) in H9c2 cells exposed to LPS were significantly enhanced by the ISO treatment. These data implied that ISO attenuated oxidative perturbation and boosted antioxidant defense in LPS-stimulated H9c2 cells.

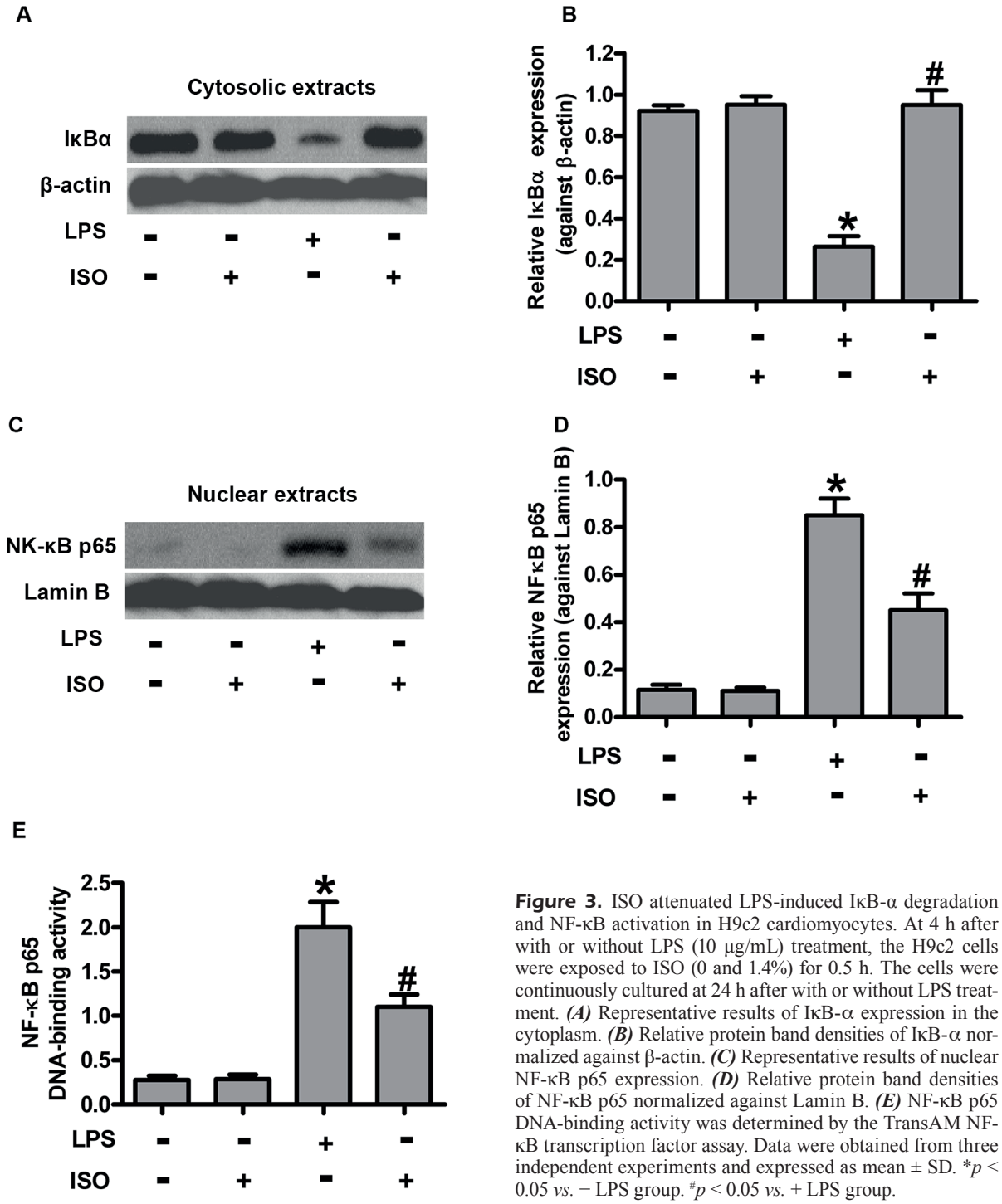

Figure 3. ISO attenuated LPS-induced IκB-α degradation and NF-κB activation in H9c2 cardiomyocytes. At 4 h after with or without LPS (10 μg/mL) treatment, the H9c2 cells were exposed to ISO (0 and 1.4%) for 0.5 h. The cells were continuously cultured at 24 h after with or without LPS treatment. ***(A)*** Representative results of IκB-α expression in the cytoplasm. ***(B)*** Relative protein band densities of IκB-α normalized against β-actin. ***(C)*** Representative results of nuclear NF-κB p65 expression. ***(D)*** Relative protein band densities of NF-κB p65 normalized against Lamin B. ***(E)*** NF-κB p65 DNA-binding activity was determined by the TransAM NF-κB transcription factor assay. Data were obtained from three independent experiments and expressed as mean ± SD. $*p < 0.05$ *vs.* − LPS group. $^{\#}p < 0.05$ *vs.* + LPS group.

ISO Inhibited LPS-induced Apoptosis of H9c2 Cardiomyocytes

To confirm the cardioprotective effects of ISO, we evaluated the apoptosis of H9c2 cells through flow cytometry, nucleosomal fragmentation, JC-1 staining, and TUNEL assays. As shown in Figure 5A, H9c2 cells challenged with LPS promoted apoptotic cell death, whereas cell apoptosis was markedly inhibited by the ISO treatment. The anti-apoptotic effects of ISO on LPS-induced H9c2 cell apoptosis were also confirmed by nucleosomal fragmentation assay (Figure 5B), analysis of

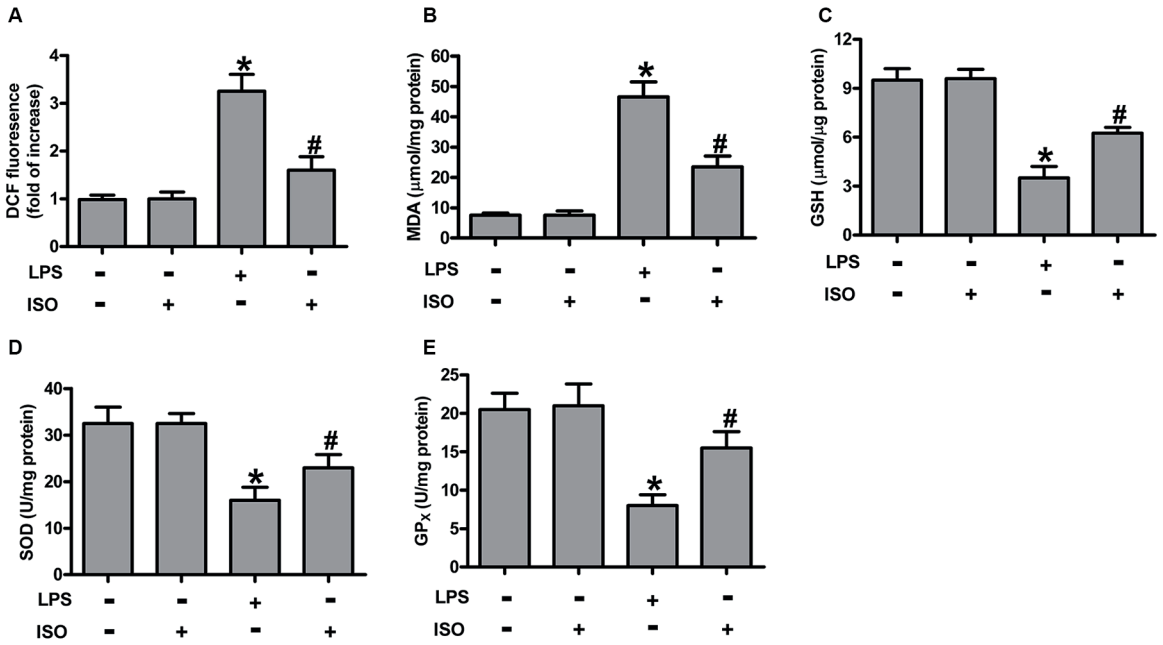

Figure 4. ISO inhibited ROS and MDA generation, as well as enhanced GSH and SOD and GPx activities in LPS-challenged H9c2 cardiomyocytes. At 4 h after with or without LPS (10 μg/mL) treatment, the H9c2 cells were exposed to ISO (0 and 1.4%) for 0.5 h. The cells were continuously cultured at 24 h after with or without LPS treatment. ***(A)*** Intracellular ROS production was represented by relative DCF fluorescence. The levels of MDA ***(B)*** and GSH ***(C)***, as well as the activities of SOD ***(D)*** and GPx ***(E)***, in the supernatants of cells with different treatments were assessed by commercial kits. Data were obtained from three independent experiments and expressed as mean ± SD. $^{*}p < 0.05$ *vs.* − LPS group. $^{\#}p < 0.05$ *vs.* + LPS group.

mitochondrial membrane potential loss (Figure 5C), and TUNEL assay (Figure 5D). To investigate the potential mechanisms of ISO-mediated anti-apoptotic effects involved in LPS-challenged H9c2 cells, we analyzed caspase-3 activity and determined the expression of apoptosis-associated proteins (i.e., procaspase-3, cleaved-caspase-3, Bax, and Bcl-2). As shown in Figure 5E, LPS-induced increase in caspase-3 activity was significantly attenuated by the ISO treatment in H9c2 cells. Furthermore, we observed that the expression of the pro-apoptotic procaspase-3, cleaved-caspase-3, and Bax was upregulated, whereas that of the anti-apoptotic Bcl-2 was downregulated in H9c2 cells treated with LPS. However, the ISO treatment reversed all changes in the expression of these proteins (Figure 5F-J). These findings demonstrated that ISO attenuated LPS-induced H9c2 cell apoptosis.

Discussion

We explored the protective effects of ISO on LPS-challenged H9c2 cardiomyocytes. ISO enhanced cell viability and reduced LDH and CK activities in H9c2 cells treated with LPS. ISO also reduced LPS-induced upregulation of proinflammatory TNF-α, IL-1β, and IL-6 levels in H9c2 cells. Moreover, ISO inhibited LPS-induced NF-κB p65 activation and DNA-binding activity in H9c2 cells. ISO inhibited LPS-induced oxidative stress and enhanced antioxidant defense in H9c2 cells. Finally, ISO prevented LPS-induced H9c2 cell apoptosis.

LPS is a major structural component of Gram-negative bacteria and a key mediator of the body's response to infection[22]; as such, this molecule is responsible for multi-organ dysfunctions, including heart failure[2]. Thus, we investigated the protective effects of ISO on heart failure by using a cell model induced by LPS exposure. As expected, the present study showed that LPS led to decreased cell viability and increased activities of LDH and CK in H9c2 cells, which are two reliable markers for the death of primary cardiac myocytes[23]. Treatment with different ISO doses (0.7%, 1.4%, and 2.1%) greatly reversed the loss of cell viability and reduced LDH and CK activities in H9c2 cells in a dose-dependent manner. These

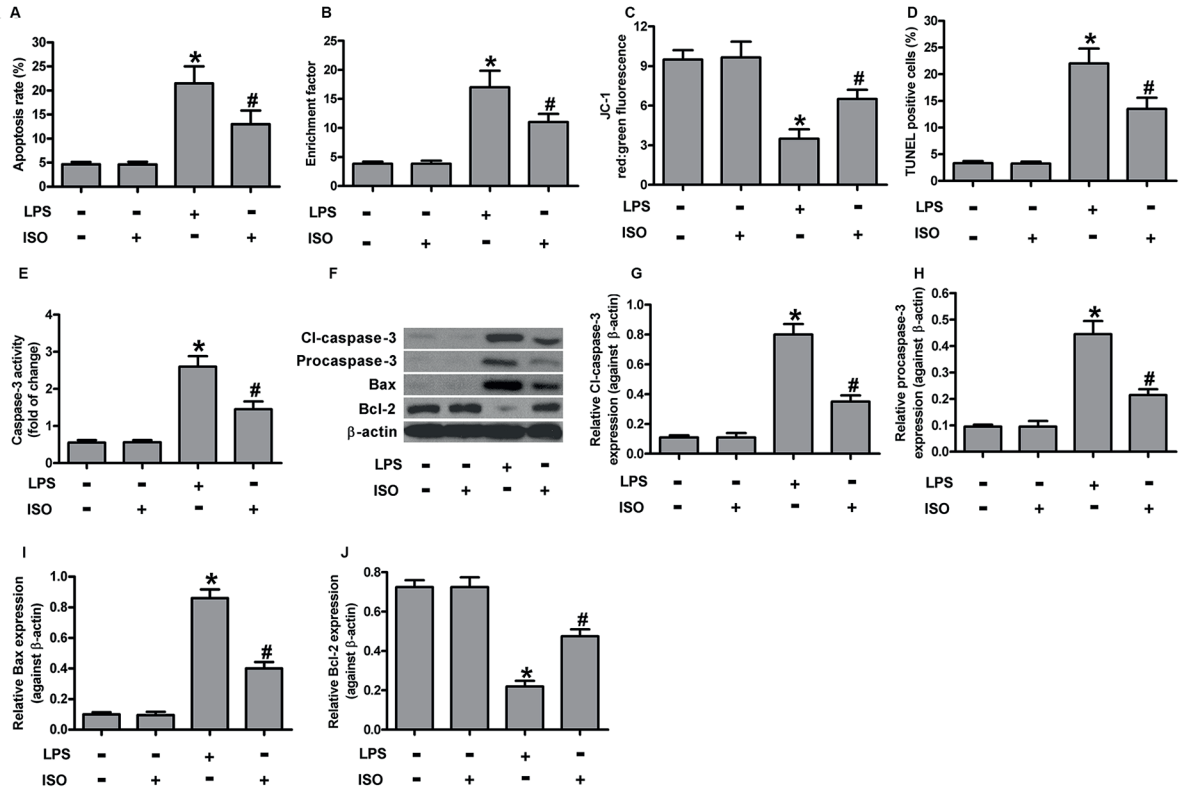

Figure 5. ISO prevented LPS-induced apoptosis of H9c2 cardiomyocytes. At 4 h after with or without LPS (10 μg/mL) treatment, the H9c2 cells were exposed to ISO (0 and 1.4%) for 0.5 h. The cells were continuously cultured at 24 h after with or without LPS treatment. ***(A)*** Apoptosis of H9c2 cells was evaluated by flow cytometry analysis. ***(B)*** Apoptotic DNA fragmentation was detected by nucleosomal fragmentation assay. ***(C)*** Changes in the mitochondrial membrane potential determined by JC-1 staining were used to assess cell apoptosis. ***(D)*** TUNEL apoptotic index was determined by calculating the ratio of TUNEL-positive cells to the total cells. ***(E)*** Caspase-3 activity was assessed using a colorimetric assay kit and expressed as fold-change relative to the control. ***(F)*** Protein expression of cleaved caspase-3, procaspase-3, Bax, and Bcl-2 was analyzed by Western blot, with β-Actin as the endogenous control. Quantitative expression levels of cleaved caspase-3 ***(G)***, procaspase-3 ***(H)***, Bax ***(I)***, and Bcl-2 ***(J)*** were normalized against β-actin. Data were obtained from three independent experiments and expressed as mean ± SD. $^{*}p < 0.05$ *vs.* − LPS group. $^{\#}p < 0.05$ *vs.* + LPS group.

results strongly suggested that ISO exerted a protective effect against LPS-induced cardiotoxicity. However, the role of ISO in LPS-induced myocardial dysfunction has not been fully investigated.

LPS-triggered inflammatory response plays a key role in septic heart failure. LPS promotes the production and release of proinflammatory cytokines, such as TNF-α, IL-1β, and IL-6, from cardiomyocytes; these proteins are early predictors of organ dysfunction and, in turn, trigger cardiomyocyte apoptosis[4,24]. Proinflammatory cytokines are major factors that impair cardiac contractile function in animals, isolated hearts, and cardiomyocytes[25,26]. TNF-α is the first cytokine induced by LPS stimulation and can trigger a signal cascade for NF-κB activation in cardiomyocytes[6]. NF-κB is a critical transcription factor in the pathogenesis of septic cardiac dysfunction[27]. Upon activation, NF-κB p65 dissociates from IκBs and translocates from the cytoplasm to the nucleus, where it may induce the transcription of proinflammatory cytokines, such as TNF-α, IL-1β, and IL-6[28]. In the present study, ISO inhibited the LPS-induced release of TNF-α, IL-1β, and IL-6 and the activation of NF-κB p65 in H9c2 cells. Therefore, the inhibitory effects of ISO on LPS-induced inflammatory responses in H9c2 cells may be involved in suppression of NF-κB activation.

Oxidative stress and consequent lipid peroxidation aggravate free radical chain reactions and activate inflammatory and apoptotic responses[29]. At the subcellular level, excessive ROS can damage nucleic acids and proteins, leading to H9c2 cell

apoptosis[30]. LPS-induced oxidative stress is characterized by excessive ROS and MDA accumulation and alteration of defense systems, such as GSH, SOD, and GPx, in myocardial tissues. This phenomenon leads to cell injury by impairment of vital macromolecules, resulting in altered membrane fluidity and mitochondrial dysfunction[31]. The balance between production and removal of ROS is essential in maintaining the redox state and homeostasis in the heart[32]. The levels of antioxidant enzymes decrease in the cardiomyocytes of decompensated heart, thereby suppressing defenses against oxidative stress[33]. ROS level is often used as an indicator of oxidative damage, and MDA is a marker for free radical-induced lipid peroxidation[34]. ROS and MDA levels increase, whereas GSH production and SOD and GPx activities decrease both in human and experimental animal studies with sepsis[34-36]. In the present study, ROS and MDA levels significantly decreased, whereas GSH production and SOD and GPx activities were significantly enhanced in LPS-challenged H9c2 cells treated with ISO. This finding indicated that the cardioprotective effect of ISO was partially dependent on its antioxidant activity.

Apoptosis is another mediator of the pathogenesis of septic cardiac dysfunction. LPS directly induces myocardial cell apoptosis via the TNF-R1-dependent pathway and by activating t-Bid to induce mitochondrion-dependent apoptotic pathways[37]. The balance between the upregulation and downregulation of the members of the pro-apoptotic (Bax and Bad) and anti-apoptotic (Bcl-xL and Bcl-2) families determines cell fate, either to undergo apoptosis or to survive. Moreover, the Bcl-2 is the upstream regulators of mitochondrial membrane potential[38]. Caspase-3 plays a central role in the execution phase of cell apoptosis. The activation of caspase-3 is governed by a series of signal transduction cascades, among which the interaction between the anti-apoptotic Bcl-2 and the pro-apoptotic Bax plays a critical role. Bcl-2 can form a heterodimer with Bax and, therefore, prevent the Bax homodimerization and sequential activation of caspase-3[39]. In the present study, reduction in the degree of apoptosis of the cells by the ISO treatment was also assayed by flow cytometry, enrichment factor analysis, JC-1 staining, and TUNEL assays in LPS-treated H9c2 cells. ISO inhibited the upregulation of pro-apoptotic proteins (procaspase-3, cleaved caspase-3, and Bax) and restored the expression of the anti-apoptotic protein Bcl-2 in LPS-challenged H9c2 cells. Thus, ISO rescued LPS-induced cell apoptosis involved in the mitochondrion-dependent apoptotic pathways.

Conclusions

We demonstrated that ISO attenuated LPS-induced injury in H9c2 cardiomyocytes by reducing proinflammatory cytokines involved in inflammatory responses and NF-κB p65 activation. Also, ISO reduced oxidative stress and increased the activities of antioxidant enzymes in LPS-challenged H9c2 cardiomyocytes. Furthermore, ISO rescued H9c2 cardiomyocytes from LPS-induced apoptosis. All these findings showed that ISO exerts cardioprotective effects via anti-inflammatory, antioxidant, and anti-apoptotic activities; thus, ISO is a promising therapeutic agent for septic cardiac dysfunction.

Conflict of Interest

The Authors declare that they have no conflict of interest.

References

1) Hotchkiss RS, Karl IE. The pathophysiology and treatment of sepsis. N Engl J Med 2003; 348: 138-150.
2) Rudiger A, Singer M. Mechanisms of sepsis induced cardiac dysfunction. Crit Care Med 2007; 35: 1599-1608.
3) Zanotti Cavazzoni SL, Hollenberg SM. Cardiac dysfunction in severe sepsis and septic shock. Curr Opin Crit Care 2009; 15: 392-397.
4) von Haehling S, Schefold JC, Lainscak M, Doehner W, Anker SD. Inflammatory biomarkers in heart failure revisited: much more than innocent bystanders. Heart Fail Clin 2009; 5: 549-560.
5) Charalambous BM, Stephens RC, Feavers IM, Montgomery HE. Role of bacterial endotoxin in chronic heart failure: the gut of the matter. Shock 2007; 28: 15-23.
6) Pahl HL. Activators and target genes of Rel/NF-kappaB transcription factors. Oncogene 1999; 18: 6853-6866.
7) Maniatis T. Transcriptional regulation of endothelial cell adhesion molecules: NF κB and cytokine inducible enhancers. FASEB J 1995; 9: 899-909.
8) Peng T, Lu X, Lei M, Moe GW, Feng Q. Inhibition of p38 MAPK decreases myocardial TNF α expression and improves myocardial function and sur-

vival in endotoxemia. Cardiovasc Res 2003; 59: 893-900.

9) Parrillo JE. Pathogenetic mechanisms of septic shock. N Engl J Med 1993; 328:1471-1477.

10) Zhou H, Yuan Y, Liu Y, Ni J, Deng W, Bian ZY, Dai J, Tang QZ. Icariin protects H9c2 cardiomyocytes from lipopolysaccharide induced injury via inhibition of the reactive oxygen species dependent c Jun N terminal kinases/nuclear factor-κB pathway. Mol Med Rep 2015; 11:4327-4332.

11) Crow MT, Mani K, Nam YJ, Kitsis RN. The mitochondrial death pathway and cardiac myocyte apoptosis. Circ Res 2004; 95: 957-970.

12) Murdoch CE, Zhang M, Cave AC, Shah AM. NADPH oxidase dependent redox signalling in cardiac hypertrophy, remodelling and failure. Cardiovasc Res 2006; 71: 208-215.

13) Singal PK, Khaper N, Farahmand F, Bello-Klein A. Oxidative stress in congestive heart failure. Curr Cardiol Rep 2000; 2: 206-211.

14) van Empel VP, Bertrand AT, Hofstra L, Crijns HJ, Doevendans PA, De Windt LJ. Myocyte apoptosis in heart failure. Cardiovasc Res 2005; 67: 21-29.

15) Mitsuhata H, Shimizu R, Yokoyama MM. Suppressive effects of volatile anesthetics on cytokine release in human peripheral blood mononuclear cells. Int J Immunopharmacol 1995; 17: 529-534.

16) Plachinta RV, Hayes JK, Cerilli LA, Rich GF. Isoflurane pretreatment inhibits lipopolysaccharide-induced inflammation in rats. Anesthesiology 2003; 98: 89-95.

17) Hofstetter C, Boost KA, Hoegl S, Flondor M, Scheller B, Muhl H, Pfeilschifter J, Zwissler B. Norepinephrine and vasopressin counteract anti-inflammatory effects of isoflurane in endotoxemic rats. Int J Mol Med 2007; 20: 597-604.

18) Lv WP, Li MX, Wang L. Peroxiredoxin 1 inhibits lipopolysaccharide-induced oxidative stress in lung tissue by regulating P38/JNK signaling pathway. Eur Rev Med Pharmacol Sci 2017; 21: 1876-1883.

19) Li JT, Wang H, Li W, Wang LF, Hou LC, Mu JL, Liu X, Chen HJ, Xie KL, Li NL, Gao CF. Anesthetic isoflurane posttreatment attenuates experimental lung injury by inhibiting inflammation and apoptosis. Mediators Inflamm 2013; 2013: 108928.

20) Wang H, Wang L, Li NL, Li JT, Yu F, Zhao YL, Wang L, Yi J, Wang L, Bian JF, Chen JH, Yuan SF, Wang T, Lv YG, Liu NN, Zhu XS, Ling R, Yun J. Subanesthetic isoflurane reduces zymosan-induced inflammation in murine Kupffer cells by inhibiting ROS-activated p38 MAPK/NF-κB signaling. Oxid Med Cell Longev 2014; 2014: 851692.

21) Sadoshima J. Redox regulation of growth and death in cardiac myocytes. Antioxid Redox Signal 2006; 8:1621-1624.

22) John E, Pais P, Furtado N, Chin A, Radhakrishnan J, Fornell L, Lumpaopong A, Beier UH. Early effects of lipopolysaccharide on cytokine release, hemodynamic and renal function in newborn piglets. Neonatology 2007; 93: 106-112.

23) Liu C, Guo W, Maerz S, Gu X, Zhu Y. 3,5-Dimethoxy-4-(3-(2-carbonyl-ethyldisulfanyl)-propionyl)-benzoic acid 4-guanidino-butyl ester: a novel twin drug that prevents primary cardiac myocytes from hypoxia-induced apoptosis. Eur J Pharmacol 2013; 700:118-126.

24) Comstock KL, Krown KA, Page MT, Martin D, Ho P, Pedraza M, Castro EN, Nakajima N, Glembotski CC, Quintana PJ, Sabbadini RA. LPS-induced TNF-α release from and apoptosis in rat cardiomyocytes: obligatory role for CD14 in mediating the LPS response. J Mol Cell Cardiol 1998; 30: 2761-2775.

25) Cain BS, Meldrum DR, Dinarello CA, Meng X, Joo KS, Banerjee A, Harken AH. Tumor necrosis factor-alpha and interleukin-1 beta synergistically depress human myocardial function. Crit Care Med 1999; 27: 1309-1318.

26) Kumar A, Thota V, Dee L, Olson J, Uretz E, Parrillo JE. Tumor necrosis factor alpha and interleukin 1beta are responsible for in vitro myocardial cell depression induced by human septic shock serum. J Exp Med 1996; 183: 949-958.

27) Li X, Luo R, Chen R, Song L, Zhang S, Hua W, Chen H. Cleavage of IκBα by calpain induces myocardial NF-κB activation, TNF-α expression, and cardiac dysfunction in septic mice. Am J Physiol Heart Circ Physiol 2014; 6: H83-843.

28) Pahl HL. Activators and target genes of Rel/NF-kappaB transcription factors. Oncogene 1999; 18: 6853-6866.

29) Finkel T, Holbrook NJ. Oxidants, oxidative stress and the biology of ageing. Nature 2000; 408: 239-247.

30) Qin J, Kang Y, Xu Z, Zang C, Fang B, Liu X. Dioscin prevents the mitochondrial apoptosis and attenuates oxidative stress in cardiac H9c2 cells. Drug Res 2014; 64: 47-52.

31) Cadenas S, Cadenas AM. Fighting the stranger-antioxidant protection against endotoxin toxicity. Toxicology 2002; 180: 45-63.

32) Wang X, Jian C, Zhang X, Huang Z, Xu J, Hou T, Shang W, Ding Y, Zhang W, Ouyang M, Wang Y, Yang Z, Zheng M, Cheng H. Superoxide flashes: elemental events of mitochondrial ROS signaling in the heart. J Mol Cell Cardiol 2012; 52: 940-948.

33) Takano H, Zou Y, Hasegawa H, Akazawa H, Nagai T, Komuro I. Oxidative stress-induced signal transduction pathways in cardiac myocytes: involvement of ROS in heart diseases. Anioxid Redox Sign 2003; 5: 789-794.

34) Ben-Shaul V, Lomnitski L, Nyska A, Zurovsky Y, Bergman M, Grossman S. The effect of natural antioxidants, NAO and apocynin, on oxidative stress in the rat heart following LPS challenge. Toxicol Lett 2001; 123: 1-10.

35) Batra S, Kumar R, Kapoor AK, Ray G. Alterations in antioxidant status during neonatal sepsis. Ann Trop Paediatr 2000; 20: 27-33.

36) Zang Q, Maass DL, Tsai SJ, Horton JW. Cardiac mitochondrial damage and inflammation responses in sepsis. Surg Infect 2007; 8: 4-54.

37) Liu CJ, Lo JF, Kuo CH, Chu CH, Chen LM, Tsai FJ, Tsai CH, Tzang BS, Kuo WW, Huang CY. Akt mediates 17 beta-estradiol and/or estrogen receptor-alpha inhibition of LPS-induced tumor necresis factor-alpha expression and myocardial cell apoptosis by suppressing the JNK1/2-NFkappaB pathway. J Cell Mol Med 2009; 13: 3655-3667.

38) Kluck RM, Bossy-Wetzel E, Green DR, Newmeyer DD. The release of cytochrome c from mitochondria: a primary site for bcl-2 regulation of apoptosis. Science 1997; 275: 1132-1136.

39) Oki M, Jesmin S, Islam MM, Mowa CN, Khatun T, Shimojo N, Sakuramoto H, Kamiyama J, Kawano S, Miyauchi T, Mizutani T. Dual blockade of endothelin action exacerbates up-regulated VEGF angiogenic signaling in the heart of lipopolysaccharide-induced endotoxemic rat model. Life Sci 2014; 118: 364-369.